

Received 15 October 2024, accepted 11 November 2024, date of publication 20 November 2024,
date of current version 9 December 2024.

Digital Object Identifier 10.1109/ACCESS.2024.3502754

RESEARCH ARTICLE

RF-Based UAV Detection and Identification Enhanced by Machine Learning Approach

YASH VASANT AHIRRAO¹, RANA PRATAP YADAV^{1,2}, AND SUNIL KUMAR¹

¹Institute For Plasma Research, Gandhinagar 382428, India

²Homi Bhabha National Institute (HBNI), Mumbai 400091, India

Corresponding author: Rana Pratap Yadav (rana.yadav@ipr.res.in)

This work is funded by the Science and Engineering Research Board (SERB), India.

ABSTRACT This paper introduces the design and implementation of an RF-based system for detecting non-cooperating unmanned aerial vehicles (UAVs). The system comprises an RF module, an automated Pan and Tilt Unit (PTU), and IoTs. The integrated RF module is highly sensitive and capable of detecting signal level up to -120 dBm in the frequency range of 2 to 6 GHz. It is designed primarily to receive frequencies used for civil and commercial UAV applications, specifically those at 2.4 and 5.8 GHz. The PTU enables azimuth rotation scanning from 0 to 360° and elevation scanning from 0 to 75°, effectively covering the surveillance space and locating the direction of RF radiation maxima. The system processes the signal data to extract key features and aiding in differentiating emitter types such as Wi-Fi, Bluetooth, or UAV control signals. Machine learning algorithms are trained to make decisions based on these extracted features. Comprehensive testing validates the system's successful performance, meeting predefined criteria. The efficacy of the system is underscored by the discernible RF fingerprints received from distinct emitters and their respective spatial parameters. In general, this paper contributes to the field of UAV detection by presenting an integrated system that combines hardware and software components, offering reliable and efficient identification and tracking of UAV signals in the presence of other RF emitters.

INDEX TERMS Internet of Things (IoT), machine learning, radio frequency (RF), signal processing, software defined radio (SDR), transceiver, unmanned aerial vehicle (UAV).

I. INTRODUCTION

In recent years, the continuous development of inexpensive embedded sensors has led to the cost-effective advancement of Unmanned Aerial Vehicles (UAVs). Consequently, the substantial growth of UAV applications has been reported in various fields including airport security, entertainment, surveillance, defense, agriculture, delivery of goods, disaster management, etc [1].

However, the widespread use and availability of UAVs have become a significant threat to the security and privacy of mankind [2]. Recent cases such as carrying unauthorized ammunition, hazardous gases, and performing unauthorized surveillance underscore the need for UAV traffic regulations [3], [4]. Some UAV manufacturers, like DJI, have incorporated geofencing software into their UAV electronics to

prevent them from entering security-sensitive areas such as government buildings and airports. However, comprehensive coverage through geo-fencing alone is impractical, especially considering concerns about system reliability. Researchers are currently focused on developing cost-effective and deployable systems for detecting non-cooperating UAVs that would aid in their neutralization [5], [6].

The detection and ranging of UAV systems pose significant challenges, primarily due to their small size, varied appearances, low flying speeds, and altitudes. Consequently, researchers are exploring various technical approaches including radar, audio, video, and RF-based surveillance [7]. However, each method shows promise for detection and localization, reliability remains a significant concern. Challenges such as design complexity, high costs, detection accuracy, limited range, etc., must be addressed. A video-based detection primarily relies on camera sensors followed by computer vision algorithms for further processing [8].

The associate editor coordinating the review of this manuscript and approving it for publication was Yanli Xu¹.

However, this technique is impeded by factors such as image background, weather conditions, and the presence of similar flying objects, especially birds. Moreover, video-based systems encounter slow detection issues due to the heavy workload of image processing tasks [9], potentially leading to missed detections. Additionally, this technique is suitable only for short ranges, typically up to 100 meters.

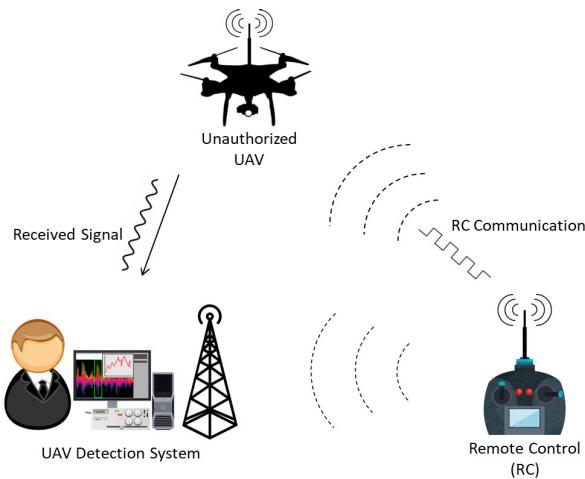


FIGURE 1. Graphical overview of UAV detection and jamming system.

Similarly, acoustic or sound-based techniques utilize arrays of microphones to extract the unique acoustic signature of UAVs [10], [11]. Typically, UAVs produce hissing or buzz-like sounds in frequencies ranging from 400 Hz to 8 kHz [12]. The angular direction can be estimated using the phase of the acquired audio signals from the UAVs. However, most of these techniques have a limited range of 25 to 30 feet [9] and are highly sensitive to environmental noise. Audio and video-based detection may be effective for detecting autonomous UAVs which are generally programmed to follow predetermined paths repetitively [13]. Radar-based detection has been one of the primary approaches for detecting and ranging flying objects [14], [15]. However, it is not suitable for tracking targets with a low radar cross-section [3]. A conventional aircraft typically induces an average Radar Cross Section (RCS) value of 426.58 m^2 (26.3 dBsm) at the lateral incidence of a millimeter-wave radar signal [16], whereas commercially available UAVs provide an average RCS value of approximately 0.02 m^2 (-16.98 dBsm) which is almost negligible ($\approx 10^{-5}$ times) compared to aircraft [17], [18], [19]. Therefore, UAVs are naturally stealthy to conventional radar.

This paper primarily exploits the RF communication signals emitted by UAV controllers for detecting and ranging non-cooperative UAVs. The design of the proposed system is discussed as follows. It includes an RF scanning receiver to capture radiated emissions from the entire aerial space. Additionally, board computers, IoT devices, and other sensors are deployed to support the system in fulfilling its computational and sensing requirements. A schematic of the proposed system is shown in Fig. 1.

RF-based system is one of the most promising methods for detecting UAVs. It has ability to detect targets without line-of-sight visibility, penetrate obstacles, and provide detailed target information makes them highly effective for monitoring and tracking UAVs in various environments. Additionally, RF-based systems offer superior range and coverage, making them ideal for detecting UAVs over large areas.

Determining the presence of UAVs involves analyzing background RF signals used in communication and control [20]. This analysis typically entails applying a discrete Fourier transform (DFT) and subsequent processing to extract key signal features [21], akin to traditional radar systems. The usual detection process involves establishing a threshold and comparing it with the energy of the received signal data stream [22]. However, this approach often yields minimal information about parameters such as signal bandwidth and carrier frequency. These parameters are necessary for the initial investigation but not sufficient for confirming the presence of UAVs because other emitters, like Wi-Fi and Bluetooth, may lie within the same range of parameters. Additionally, the localization of UAVs remains a concern that requires further investigation.

Recent investigations have extracted key features of UAV signals, particularly related to encryption and communication protocols, through demodulation and time-domain analysis. Since communication signals exhibit specific patterns in the time domain, these approaches have found to be more effective than earlier methods. Lv et al. [23] investigated frequency hopping pattern commonly found in UAV communication signals and established an auto-correlation function using frequency (side-band) cancellation. This enhanced the baseband signal, highlighting its various features. However, the baseband signal has many similarities with Bluetooth signals, which may cause false detection due to coexisting signal interference. Addressing the challenges posed by coexisting signals, Yang et al. [24] presented a comprehensive approach to classify signals into UAV, WiFi, or Bluetooth categories. Machine learning algorithms, including pre-trained CNN models (e.g., SqueezeNet), Feature Engineering Generator (FEG), and Multichannel Deep Neural Network (MC-DNN), aim to detect UAV presence and classify flight modes based on measurements associated with IQ samples of multiple re-emitters [25], [26]. Furthermore, Ozturk et al. [27] applied CNNs trained with RF time-series images and spectrograms to classify different UAV controllers under varying signal-to-noise ratios (SNR). Additionally, Medaiyese et al. [28] utilize wavelet transform analytics to extract unique features from RF signals. Also apply machine learning for the detection and identification of re-emitter types, resulting in significant accuracy improvements [29].

Although significant improvements in UAV detection and identification have been reported in recent years, it remains an active area of research due to ongoing challenges, primarily related to reliability, portability, limited range, and localization. Localization heavily depends on the relative

signal strength and its directivity. Control signals from remote controllers (RC) vary for each type of UAV, presenting a significant challenge in establishing reference datasets for localization. Earlier investigations have failed to address localization issues due to the lack of reference signal data. Additionally, most of these studies were based on proof-of-concept models that utilized lab-based equipment for data collection, limiting their ability to address current challenges due to hardware constraints. To the encounter the earlier issues we have worked with various aspect which has been discussed as follows,

- 1) **Integrated System:** Developed system present an integrated module which incorporates real-time signal processing capabilities, allowing it to detect, trace, and localize UAVs as they move within the surveillance zone.
- 2) **Enhanced Detection Range:** Signal processing adopts a multidimensional approach to extract key features essential for the unique identification of UAV signals. By analyzing the signal alongside its frequency hopping pattern and embedding its distinctive fingerprint, this approach significantly enhances detection capabilities. **Key steps, including discrete wavelet transforms and multi-resolution analysis,** allow for efficient down-sampling and demodulation, enabling the extraction of critical signal characteristics such as bandwidth, symbol duration, and frequency variance. This method effectively boosts sensitivity, enabling signal detection at levels as low as -120 dBm, with a detection range of up to 300 meters, the highest ever reported in the literature.
- 3) **Effective Classification:** The system integrates advanced machine learning techniques, such as Gaussian Naive Bayes (GNB), for accurate UAV classification with up to 99.6% detection accuracy, even in low SNR conditions.
- 4) **Hardware Reliability:** In terms of reliability, the design is tailored to meet specific requirements, focusing on an efficient and portable RF receiver module, along with automation, computational, and control capabilities. Component selection is driven primarily by technical needs, ensuring availability and compatibility for seamless integration into the design. While access to high-end hardware is limited, we mitigate this through effective signal and data processing techniques. For instance, the sample rate of the general-purpose SDR in our system is capped at 42 MSPS, whereas lab-based equipment like Vector Network Analyzers (VNA), oscilloscopes, and high-end SDRs used in previous studies offer gigahertz-range sampling rates.

Detection range and accuracy is presented in Table: 1 in perspective comparison with earlier findings.

The overall proposed system is mounted on an automated Pan and Tilt Unit (PTU) which continuously scans the aerial space from 0° to 360° in azimuth and 0 to 75° in elevation

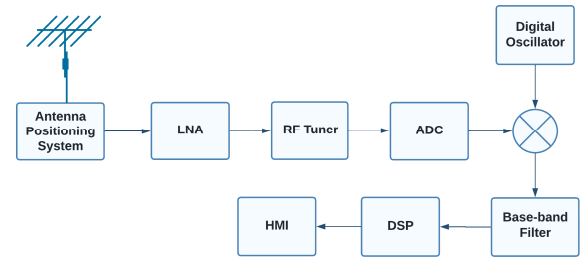


FIGURE 2. Block diagram of RF scanning receiver.

using the PTU to capture RF re-emissions typically in the range of 2 to 6 GHz. A computing board, sensors, and controllers are all together responsible for monitoring and controlling of PTU. Also provides information on the angular position of remitters. Whereas the received signal undergoes processing to extract key features for differentiating signal types and training machine learning models. Specifically, a class of UAVs utilizes remote controllers (RC) with Automatic Frequency Hopping Digital Systems (AFHDS), where communication involves rapidly switching between multiple channels to prevent jamming. The FHSS features can be utilized for identifying UAVs of this particular class. The system is tested using various datasets, including one with 120 signals from different emitters. This detection model achieves 99.6% accuracy across Gaussian Naive Bayes, Neural Network (NN), and Support Vector Machine (SVM) models, successfully classifying emitter types, particularly in outdoor environments. The system has demonstrated its capability to detect UAVs and decode RC controller frequency hopping based on spectral analysis.

II. SYSTEM DESIGN

The block diagram of the RF-based system design is shown in Fig.2. It can be divided into the following subsystems, (II-A) an RF scanning receiver to capture the control signal of the UAVs, and (II-B) an Antenna Pan and Tilt Unit (PTU) along with IoTs integrated for signal and data processing. The details of the subsystems are discussed as follows,

A. RF SCANNING RECEIVER

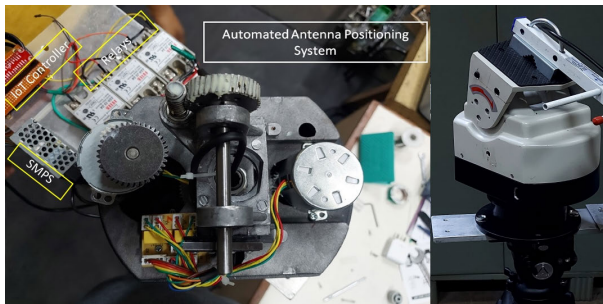
The RF scanning receiver architecture has been meticulously engineered to serve as a versatile platform for experimental endeavors, comprising several pivotal components. These include a Directional Grid Parabolic Antenna, a Low-Noise Amplifier (LNA), and an Analog Device-based Software-Defined Radio (SDR) equipped with a Xilinx Zynq Z-7010 FPGA and a ZX60-63GLN+.

The Grid Parabolic Antenna utilized in our experiments exhibits a gain of 24 dBi and operates within a frequency range of 2400 MHz to 2500 MHz. It features a horizontal beamwidth of 9.5 degrees and a vertical beamwidth of 13 degrees, with a maximum power handling capacity of 100 watts. Although the receiver is optimized for the 2 GHz to 6 GHz range, our experiments conducted at 2.45 GHz

TABLE 1. Detection accuracy of UAVs based on ML models.

Sr. No.	ML Methods	SNR	Accuracy(%)	Range (Meters)	Reference
1	kNN	25 dB	97.30	200	[30]
2	DNN	10 dB	84.5	-	[31]
3	DNN	10 dB	97.5	-	[24]
4	ANN	Not mentioned	75.0	-	[32]
5	GNB	5 dB	99.6	300	Our work

demonstrated effective performance, and the system also proved functional at 5.8 GHz. Nevertheless, for directional determination, the antenna is the chosen instrument, although it may be substituted with a grid or horn antenna for superior directivity in future iterations.

**FIGURE 3.** Photograph of PTU.

The SDR module exhibits an impressive frequency coverage extending from 325 MHz to 3.8 GHz, coupled with a flexible channel bandwidth tunability ranging from 200 kHz to 20 MHz. Housing the AD9363 chipset, the SDR integrates a 12-bit ADC and DAC, facilitating seamless operation in both half-duplex and full-duplex modes. It effectively supports Time Division Duplex (TDD) and Frequency Division Duplex (FDD) operations, ensuring versatility in experimental setups.

Additionally, the SDR module is embedded with dual transmitters capable of synthesizing signals with high precision. Critically, it has a step size of 2.4 Hz, a low noise floor of ≤ -157 dBm/Hz, and an insignificant Transmit Error Vector Magnitude (EVM) of -34 dB. It can be provisionally utilized for signal synthesis for jamming applications.

The LNA within the system operates within the frequency range from 1800 MHz to 6000 MHz, offering a maximum input power of 10 dBm. It has a wide-band flat gain of 29.8 dB at 2.5 GHz, with a variance ± 1.6 dB typ. over the 2.5 to 5 GHz range.

This integrated architecture provides an efficient and flexible RF scanning subsystem, combining advanced SDR capabilities with high-performance amplification and precise signal direction.

B. PAN AND TILT UNIT (PTU)

The antenna positioning system is engineered with a motorized rotation mechanism, to achieve azimuth and elevation movement controlled by a solid-state relay module (SSR). An IoT-based computing board, named Raspberry Pi offers precise control over its orientation, operating within the range

of 0° to 360° in azimuth and 0° to 75° in elevation, and the system's functionality is extended through programmable features. Custom written programs on the Raspberry Pi enable users to switch between scan and position modes. Moreover, leveraging the capabilities of the Raspberry Pi, the system can be operated remotely over the network, enhancing its accessibility and usability for users located at varying distances from the antenna setup. With a payload capacity of 5 Kg, the pan-and-tilt unit can accommodate various antennas and equipment. In particular, the azimuth rotation resolution is set at 10° per second, while the elevation operates at 2° per second, ensuring precise positioning capabilities for the antenna. This PTU integrates motorized control, Internet of Things (IoT) devices, and the programmability of the controller to provide a reliable and adaptable solution for antenna positioning.

III. SIGNAL DATA RECEPTION AND PRE-PROCESSING

Our investigation primarily concentrates on analyzing the signal characteristics of both Unmanned Aerial Vehicles (UAVs) and Remote Control (RC) controllers. It's essential to note that we use these terms interchangeably throughout our study. These signals are primarily utilized for communication, control, and data transfer (uplink or downlink). The characterization of signals can be made based on frequency bandwidth, modulation/demodulation, symbol rate, and communication protocol [33]. These all parameters collectively present the unique feature of a signal. This uniqueness is sometimes referred to as an RF fingerprint. Analysis of the RF fingerprint provides useful information for the classification of the type of radiator [34].

The receiver is set in the range of 2 to 6 GHz UAV controller frequency, mainly 2.4 GHz and 5.8 GHz. This is also allocated for WiFi, Bluetooth, and other commercial use [39]. Therefore, UAV detection needs serious investigation regarding the classification of radiator types [35]. Various signal processing steps to extract the key features of received signals are established to differentiate the re-emitter type [36]. Details of the above discussed as follows,

- Initially, the scanning receiver captures signal data, including WiFi and Bluetooth signals, with a sampling rate of 60 MHz. This rate ensured the reception of signals with a bandwidth ≤ 20 MHz, preserving their essential features. The received data plot, depicted in Fig 4, illustrates this capture.
- In the subsequent phase, the UAV control signal was introduced along with WiFi, Bluetooth, and other noise interference. The raw composite signal underwent demodulation for further analysis of its time and

frequency domain parameters. The resulting plot is shown in Fig. 4. Several new signal peaks have appeared as RC is turned on. It has been analyzed further for different features like channel bandwidth, average signal strength, FFT coefficients, etc.

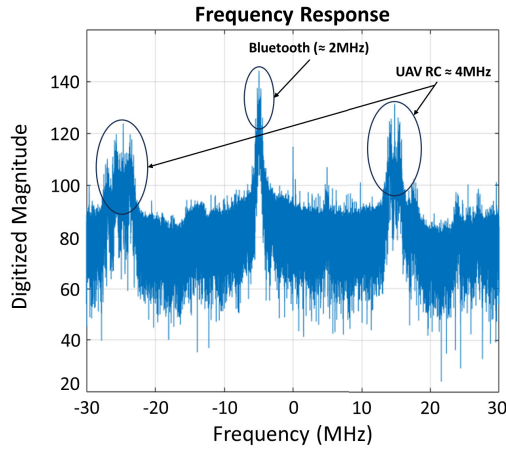


FIGURE 4. Bandwidth analysis.

A. CLASSIFICATION AND DETECTION

Further signal processing has been planned for extracting key features to get around conclusive steps, especially for the detection of UAVs. Based on our investigation, a few criteria have been fixed for classification and detection which are mentioned as follows,

- **Signal Bandwidth:** In general WiFi, Bluetooth and RC communication signals are GFSK modulated. Its demodulation presents data bandwidth which may be different for each remitter. It is highest for WiFi i.e., ≥ 10 MHz, and lowest for Bluetooth which is ≤ 2 MHz whereas RC Bandwidth is slightly greater than Bluetooth and found somewhere within 3 to 4 MHz.
- **Symbol Duration:** In general, the symbol duration correlates directly with the transfer data bit rate. For WiFi, it is expected to range from approximately $4\mu s$ to $12\mu s$, while for Bluetooth, it is around $0.5\mu s$, and for UAV communications, it is approximately $2\mu s$.
- **Frequency Variance:** In most of the UAV controllers modulation frequency hops between multiple frequency bands and is rooted through different communication channels. This particular is adopted to prevent it from other signal interference like WiFi, Bluetooth, jamming signals, etc. It prominently differentiates RC signals from others. This difference can be analyzed through frequency variance.
- **Statistical Features:** RC signals are purposefully originated to ensure communication for control and navigating the UAVs. Its statistical features can be different from the other emitters which are solely made for data communication. These statistical features can be analyzed using an Machine Learning (ML) Classifier to identify the UAV signals.

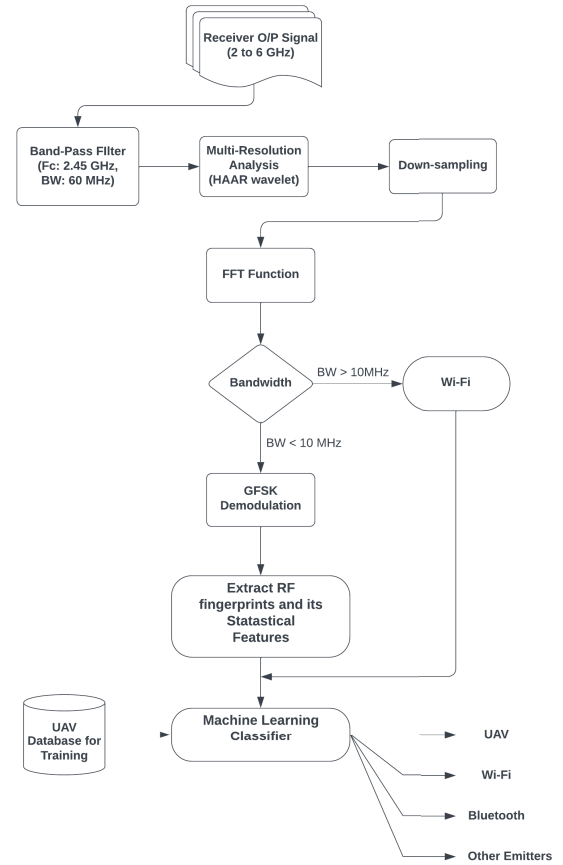


FIGURE 5. Flowchart for signal processing steps and classification.

The Fig.5 shows a flowchart presenting signal processing steps for UAV detection. Receiver outputs are passed through different signal processing stages, filtering, down-sampling, FFT, and demodulation. Afterward, signal data is available for analysis of different parameters based on discussed criteria.

The important stages like down-sampling and demodulation are explained as follows,

Down-sampling: It has been performed to reduce the sample size mainly to get optimum processing speed with a minimum hardware requirement. Signal down-sampling and multi-resolution decomposition have been executed using HAAR wavelet transform (DWT multi-resolution) [15] shown in Fig.6.

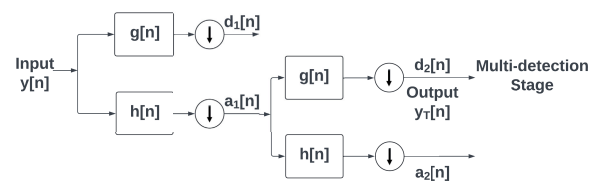


FIGURE 6. Signal flow graph representation for two-level discrete Haar wavelet transform.

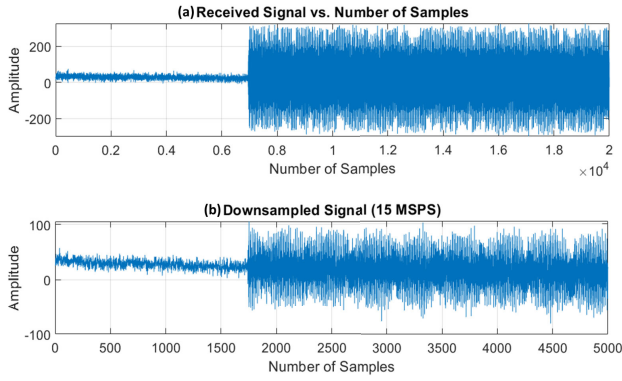


FIGURE 7. (a) Receiver signal, $y[n]$, (b) Down-sampled signal $y_T[n]$.

The first two-level Haar transform splits the input RF data into low- and high-frequency components using half-band low-pass ($h[n]$) and high-pass ($g[n]$) filters. The resulting outputs undergo dyadic decimation to produce approximate coefficients ($a_1[n]$) and detail coefficients ($d_1[n]$) at the first level. These $a_1[n]$ coefficients then undergo further decomposition, resulting in $d_2[n]$ coefficients, which are the final output ($y_T[n]$). The transformed output $y_T[n]$ is then fed into a multistage detection system. As we move from left to right in the signal flow graph, a coarser representation of the original RF data is obtained. Due to successive down-sampling, the output RF data has fewer samples, reducing computational complexity. Multi-resolution analysis is particularly beneficial for detecting weak signals amidst background noise and removing signal bias, thus improving detection accuracy. The sampled RF signal from the controller is illustrated in Fig. 7.

Demodulation: Further demodulation steps are performed to get an analysis regarding frequency deviation, symbol duration and Frequency Hopping Spread Spectrum (FHSS). These variables are the parameters of GFSK/FSK modulation. Frequency deviation imposed various peaks on the frequency spectrum with different amplitude. The UAV communication and Bluetooth signal peaks are superimposed on the WiFi band of ≥ 10 MHz because of their stronger amplitude and narrower bandwidth with 2 to 4 MHz as shown in Fig. 4. Therefore, UAV control and Bluetooth signal induces significant levels of variance with the wifi signal amplitude. Now, selection of signal peaks has been made based on bandwidth ≤ 10 MHz (Bluetooth and UAV) for further processing.

In addition to GFSK modulation, UAVs employ the FHSS technique. FHSS involves rapidly switching between different frequencies within a specific bandwidth to enhance signal robustness and reduce interference. In analysis, the combined use of GFSK modulation and FHSS aids in distinguishing UAV signals from Wi-Fi and Bluetooth signals.

The Bluetooth GFSK / FSK signal is known to be transmitted in burst consisting of M data bits (dm) $\in [-1, +1]$ each bit having a period T_b and average energy per

bit E_b [37]. A general model for such a signal is given as,

$$s(t) = \sqrt{\frac{2E_b}{T_b}} \cdot \cos(2\pi f_o t + \phi(t, \alpha) + \phi_o) + n(t) \quad (1)$$

where, $\phi(t, \alpha)$ is a phase modulating function, ϕ_o is an arbitrary phase constant, f_o is the operational frequency, and $n(t)$ is the channel noise component. The zero-crossing demodulator considered herein for Bluetooth interference detection can detect the time instants at which the signal $s(t)$ is equal to zero and has a positive slope, that is, the zero crossings. When a Bluetooth device transmits at the basic rate using the standard GFSK/FSK modulation, one symbol represents one bit. Therefore, the time interval between consecutive zero-crossings is a measure of the symbol duration of the Bluetooth signal.

On the other hand, the symbol duration refers to the minimum time interval observed within the signal pulse. It mainly counts zero crossovers of pulse amplitude. All the Bluetooth signals have a symbol duration of $0.5\mu s$ and a frequency deviation of less than 350 kHz. Frequency deviation and symbol duration can be used as features in a simple maximum likelihood classifier for identifying Bluetooth interference signals. If the detected signal is not from a Bluetooth interference source, it is presumed to be an emission from a UAV controller. Further steps involve the collection of data for the training and automation using ML algorithms. Here data is analyzed with and without a UAV control signal.

The demodulated signal without UAVs is shown in Fig. 8 where $s(f)$ and $s(t)$ present frequency and time domain, respectively, in Fig. 8.a.(i) and 8.a.(ii). Fig 8.a.(iii) and 8.a.(iv) consecutively presents the same as shown in 8.a.(ii) with better resolution, ET and ETM . It is termed as energy transient and presents greater details about signal transients, especially the symbol duration and rate. Similarly in Fig. 8.b corresponding terms are shown denoted as $S_w(f)$, $S_w(t)$, ET_w , and ETM_w .

For a perspective comparison, the frequency peaks in $S_w(f)$ signify the hopping signals and confirm the presence of the UAV. further magnification of the $S_w(t)$ shows time-varying modulating patterns which are not found in case $S(t)$. In addition, further analysis will provide additional information related to symbol duration, rate, and other statistical parameters that can be useful for training an efficient ML model. Our developed model considers various levels of parameters based on signal features like Bandwidth, symbol duration, frequency variance, entropy, etc.

B. UAV DETECTION USING RF FINGERPRINT

The earlier analysis presents the pre-processing steps where different parameters have been finalized to characterize the signal and classify it for RF fingerprint. The term RF fingerprint describes the reference dataset obtained from training the ML model using existing UAVs, WiFi, and Bluetooth signals. The ML model has been created using an

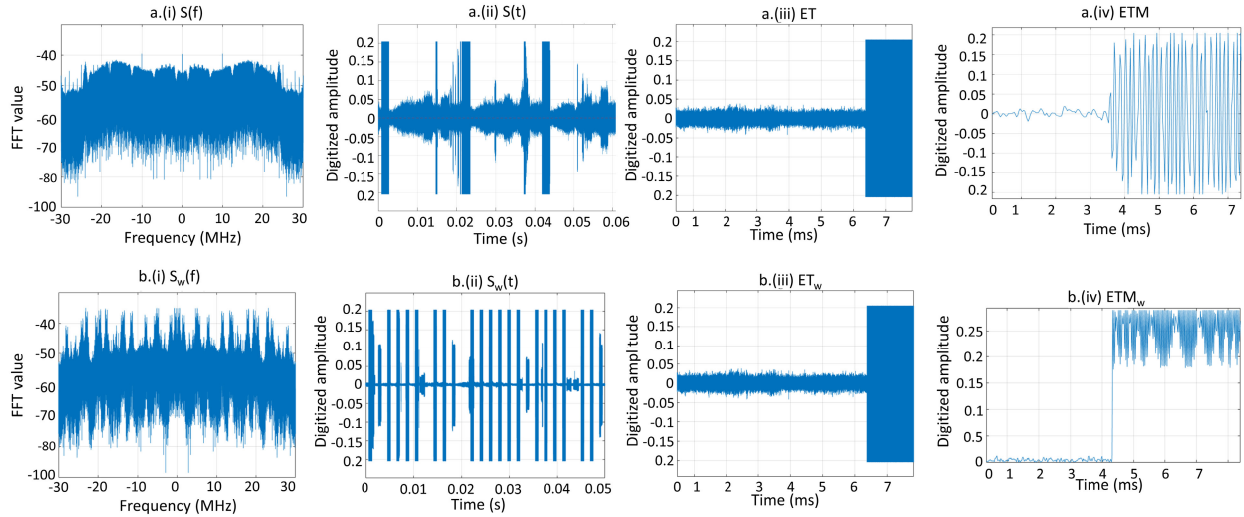


FIGURE 8. Demodulated Signal a) Without UAV signal i) in frequency domain $S(f)$ ii) in time domain $S(t)$ iii) Energy transient ET (iv) Magnified view of $ET(ETM)$ b) With UAV signal i) in frequency domain $S_w(f)$ ii) in time domain $S_w(t)$ iii) Energy transient ET_w (iv) Magnified view of $ET_w(ETM_w)$.

ML classifier. It gets input from the signal data and classifies it based on different features. The representation used for signal feature analysis is called the frequency spectrum method. It is a discrete-time short-time Fourier transform (STFT) of the square magnitude of the signal. Having the squared magnitude of the resulting complex values provides the power spectral density (PSD) of the signal. It provides details of the frequency content of a signal over time by analyzing Fourier Transform in short segments of the signal. Also provides different derivatives in terms of features shown in table 2 which are utilized further for classification and detection. The STFT signal is described as follows,

$$S(f, t) = \left| \sum_{n=0}^{N-1} x(n) \cdot w(n-t) \cdot e^{-j2\pi fn} \right|^2$$

where,

- $S(f, t)$ is the frequency spectrum of the signal at frequency f and time t .
- $x(n)$ is the signal in the time domain.
- $w(n-t)$ is the window function applied to the signal segment.
- N is the number of samples in each segment.
- $e^{-j2\pi fn}$ represents the complex sinusoid at frequency f .

Fig. 9 displays the results of the Minimum Redundancy Maximum Relevance (MRMR) ranking applied to 12 features extracted from UAV controllers, WiFi, Bluetooth (BT), and interference signals. The MRMR algorithm is utilized to rank features based on their discriminative power while considering redundancy among them. This aids in identifying the most informative features for subsequent analysis.

Upon examination of Fig. 9, it becomes evident that MRMR ranks the features according to their weight values. Notably, the standard deviation and entropy emerge as the most discriminative features within the feature set. Following

closely is the kurtosis, which characterizes the tailedness of the energy trajectory curve. Subsequently, skewness and meanness are identified as significant features. These findings are instrumental in guiding machine learning (ML) algorithms to discard less important features, therefore potentially improving classification performance. By reducing the likelihood of overfitting through the elimination of less significant features, ML algorithms can still achieve robust classification accuracy. Moreover, the reduction in feature dimensionality leads to substantial computational savings during both the training and testing phases, particularly beneficial for large-scale classification tasks.

The features extracted from UAV controllers, WiFi, Bluetooth, and interference are used to train five different ML algorithms: k-Nearest Neighbors (kNN), Gaussian Naive Bayes (GNB), MSupport Vector Machine (SVM) and neural networks (NN). More details can be found in [38].

The different combinations of the feature have been plotted and are shown in Fig. 10. In the given figure signals from the different emitters are mapped using scatters. It clearly shows the UAV and non-UAV signals belong in different group of scatters with significant gaps.

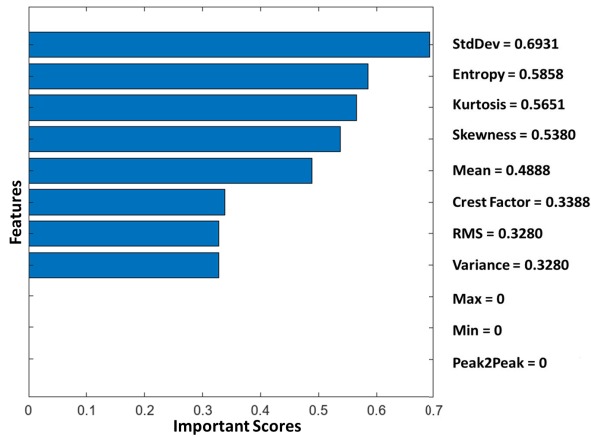
These results (Table 3) demonstrate that the Naive Bayes model performed the best in terms of accuracy, achieving 99.6%. However, the Neural Network model exhibited the highest prediction speed at 11251.7054 obs/sec, making it efficient for real-time UAV detection applications. The choice of model can be based on the specific requirements of the UAV detection system, considering factors such as accuracy, cost, and prediction speed.

IV. TESTING AND VALIDATION

The experiments were conducted in an anechoic chamber and an outdoor environment to evaluate system performance under controlled and real-world conditions.

TABLE 2. Signal extraction feature formulas for ML classifier.

S. No.	Formula
1	Mean = $\frac{1}{N} \sum_{i=1}^N x_i$
2	Variance = $\frac{1}{N} \sum_{i=1}^N (x_i - \text{Mean})^2$
3	Std Deviation = $\sqrt{\text{Variance}}$
4	Median = middle value of x_1, x_2, \dots, x_N
5	Minimum = $\min(x_1, x_2, \dots, x_N)$
6	Maximum = $\max(x_1, x_2, \dots, x_N)$
7	Skewness = $\frac{\frac{1}{N} \sum_{i=1}^N (x_i - \text{Mean})^3}{(\frac{1}{N} \sum_{i=1}^N (x_i - \text{Mean})^2)^{3/2}}$
8	Kurtosis = $\frac{\frac{1}{N} \sum_{i=1}^N (x_i - \text{Mean})^4}{(\frac{1}{N} \sum_{i=1}^N (x_i - \text{Mean})^2)^2}$
9	Entropy = $-\sum_{i=1}^N p(x_i) \log p(x_i)$
10	Crest Factor = $\frac{\text{Peak Value}}{\text{RMS Value}}$
11	RMS = $\sqrt{\frac{1}{N} \sum_{i=1}^N x_i^2}$
12	Peak-to-Peak = Maximum – Minimum

**FIGURE 9.** Feature importance scores using MRMR algorithm.

A. INDOOR TESTING SETUP

Indoor testing was performed in an anechoic chamber to minimize external RF interference, providing a controlled environment for initial system calibration and testing. The setup featured a grid antenna mounted on a tripod and connected to an IoT box housing the necessary electronics and interfaces for signal processing. A UAV remote control (RC) was positioned within the chamber to simulate UAV signals. During testing, the grid antenna was oriented towards the UAV RC, which was activated to emit RF signals. The system executed real-time signal processing to detect the UAV RC, with the pan and tilt unit automatically adjusting the antenna orientation to maintain signal lock.

B. OUTDOOR TESTING SETUP

Outdoor tests were conducted to evaluate the system's performance in a real-world environment with varying conditions and potential interference sources. The setup for outdoor testing as shown in fig 11 included the same grid

antenna and pan and tilt unit, connected to an IoT box and a Software Defined Radio (SDR) for flexible signal processing and data collection. The grid antenna and pan and tilt unit were mounted on a tripod, and the UAV RC was placed at various distances within the outdoor test area. A computational system, consisting of a laptop with a developed detection program, was used for real-time signal processing and analysis.

In the outdoor tests, the grid antenna was initially oriented towards the UAV RC, which was then activated and moved to different locations to test various operational scenario where response of RC activation and deactivation has been recorded by the system accurately. The system continued to perform real-time signal processing to detect the UAV RC, with the pan and tilt unit automatically adjusting the antenna orientation to maintain signal lock. Data on detection range, accuracy, signal strength, and system response time was collected throughout the testing.

C. REAL-TIME DETECTION ANALYSIS

Figure 12 illustrates the real-time detection analysis. Sub-figure (a) displays the Power Spectral Density (PSD) over time, showing variations in signal strength as the UAV RC was activated and moved. Sub-figure (b) represents the detection results, where a value of 1 indicates UAV detection and a value of 0 indicates the absence of UAV signals. The system demonstrated consistent and accurate detection throughout the test duration, with distinct periods of UAV signal presence and absence clearly identifiable.

D. SIGNAL STRENGTH VS. RANGE

Figure 13 presents the relationship between signal strength and range. As expected, the digitized amplitude of the UAV signals decreases with increasing distance from the signal source. The trendline in the figure indicates the overall pattern of signal attenuation, which aligns with theoretical expectations. The data points illustrate the measured signal strength at various distances, confirming the system's capability to detect UAV signals up to 300 meters. The system can calibrate signal strength depreciation for the range calculation using the trendline data. The range is an important parameter for the localization of UAV re-emitters.

E. OVERALL SYSTEM PERFORMANCE

The results from the outdoor tests confirmed the system's capability to detect and localize UAVs at a range of up to 300 meters using low-cost and reliable equipment. The system demonstrated robust performance in varied and dynamic outdoor environments, and the automated pan and tilt unit effectively tracked the UAV RC, providing continuous and accurate localization.

The experiment involved capturing RF signals from UAV controllers, mobile Bluetooth devices (smartphones), and a Wi-Fi router. To validate the developed system, an indoor setup was planned, with WiFi, Bluetooth, and UAV RC placed around the detection system. The system initially analyzed

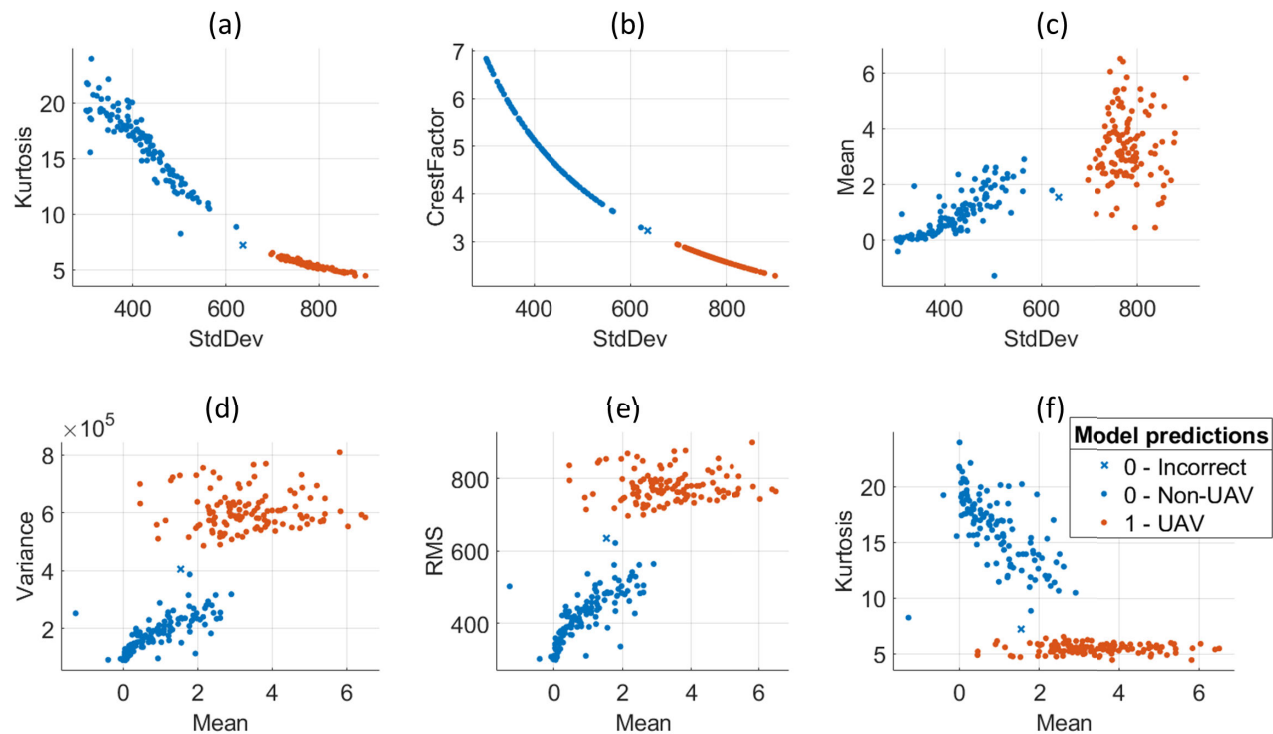


FIGURE 10. ML classifier's scatter plot a) stdDev vs Kurtosis b) stdDev vs Crest Factor c) stdDev vs mean d) mean vs variance e) mean vs RMS f) mean vs kurtosis.

TABLE 3. Perspective comparison of performance based on ML model.

S. No.	Model Type	Accuracy (Validation) %	Total Cost (Validation)	Prediction Speed (obs/sec)
1	Efficient Linear SVM	99.2	2	5718.002416
2	Naive Bayes	99.6	1	2640.560327
3	SVM	98.75	3	6416.63191
4	KNN	99.6	1	5805.641632
5	Neural Network	99.2	2	11251.70534

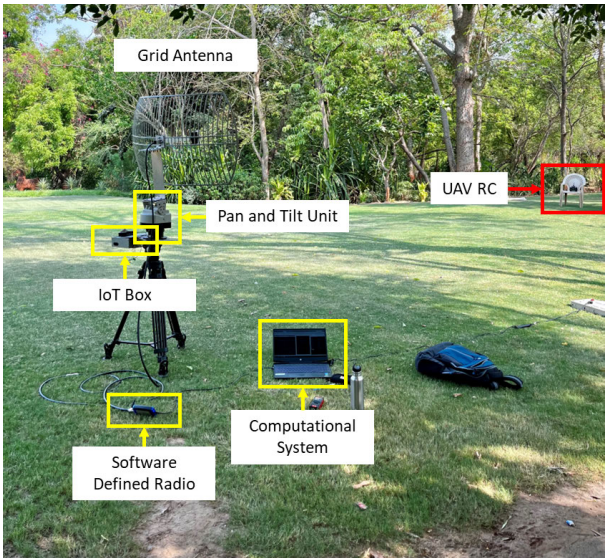


FIGURE 11. Photograph of outdoor test setup.

and classified signals for each type. Upon identification, it scanned from 0° to 360° in azimuth to trace the intensity

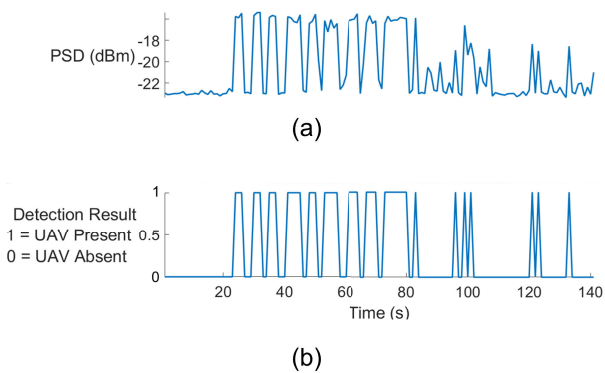


FIGURE 12. Plot for Real-Time UAV detection (a) PSD in different Range (b) Detection Plot.

of each signal type. Test results revealed three emitter types: WiFi, Bluetooth, and UAV RC. Each emitter type was identified and traced for signal intensity maxima, with the system capable of tracking multiple single-emitter types simultaneously. Furthermore, it could be set exclusively in UAV tracking mode. Photographs of the complete setup and

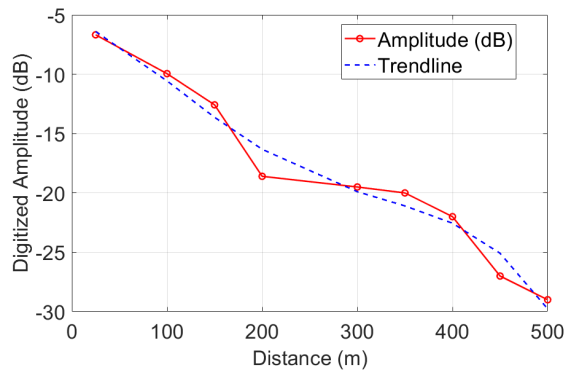


FIGURE 13. Signal Strength vs Range.

test results are provided in Figures 11, 12, and 13, respectively, which depict the direction of the emitter and the strength of the signal.

UAV controllers typically transmit control signals in the 2.4 GHz and 5.8 GHz frequency bands. Enhancements to the RF surveillance system could involve employing high-gain receive antennas and low-noise power amplifiers (LNAs). The receiver antenna continuously monitors the environment for RF signals. During both training and testing phases, real-time data capture occurred, with captured data segmented into specific-duration windows and automatically saved for post-processing. To ensure accurate detection of RF signals, the window length was set sufficiently small to prevent noise signal dominance over signal transitions. The data were partitioned into 70% for training (55% for training, 15% for cross-validation) and 30% for testing. The test data was put aside while cross-validation was performed during training to mitigate over-fitting and bias. This approach ensured robustness and accuracy in the training of machine learning models.

V. CONCLUSION

An RF-based system design and development presented in this paper offer a solution for UAV detection using advanced signal processing techniques and machine learning algorithms. A highly sensitive receiver facilitates a versatile platform for receiving signals with very low intensity of -120 dBm in the range of 2 to 6 GHz. Combined with an antenna pan and tilt unit (PTU), it enables the scanning of surveillance space from 0° to 360° in azimuth and from 0° to 75° in elevation effectively for RF signal intensity. Further, pre-processing steps, including demodulation and feature extraction, allow for the identification of key parameters such as signal bandwidth, symbol duration, frequency variance, and statistical features, sorting the received signals based on different features for fingerprint analysis. Utilizing machine learning models such as kNN, GNB, SVM, and NN, the system achieves high accuracy ranging from 98.75% to 99.6% in classifying signals based on RF fingerprints and detecting UAVs. Testing and validation in an indoor setup demonstrate the system's ability to successfully detect, trace, and track UAV signals, showcasing its effectiveness in

real-world scenarios. The flexibility, accuracy, and speed of the system make it a valuable tool for applications such as security, surveillance, and UAV traffic management. Overall, this research contributes to the field of RF-based UAV detection by providing an integrated system that combines hardware and software components to deliver reliable and efficient performance in UAV signal identification and tracking.

REFERENCES

- [1] S. Hussain, S. A. Chaudhry, O. A. Alomari, M. H. Alsharif, M. K. Khan, and N. Kumar, "Amassing the security: An ECC-based authentication scheme for Internet of Drones," *IEEE Syst. J.*, vol. 15, no. 3, pp. 4431–4438, Sep. 2021.
- [2] I. Guvenc, F. Koohifar, S. Singh, M. L. Sichitiu, and D. Matolak, "Detection, tracking, and interdiction for amateur drones," *IEEE Commun. Mag.*, vol. 56, no. 4, pp. 75–81, Apr. 2018.
- [3] I. Güvenç, O. Ozdemir, Y. Yapici, H. Mehrpouyan, and D. Matolak, "Detection, localization, and tracking of unauthorized UAS and jammers," in *Proc. IEEE/AIAA 36th Digit. Avionics Syst. Conf. (DASC)*, Sep. 2017, pp. 1–10.
- [4] B. Nassi, A. Shabtai, R. Masuoka, and Y. Elovici, "SoK—security and privacy in the age of drones: Threats, challenges, solution mechanisms, and scientific gaps," 2019, *arXiv:1903.05155*.
- [5] S. Park, H. T. Kim, S. Lee, H. Joo, and H. Kim, "Survey on anti-drone systems: Components, designs, and challenges," *IEEE Access*, vol. 9, pp. 42635–42659, 2021.
- [6] G. Ding, Q. Wu, L. Zhang, Y. Lin, T. A. Tsiftsis, and Y.-D. Yao, "An amateur drone surveillance system based on the cognitive Internet of Things," *IEEE Commun. Mag.*, vol. 56, no. 1, pp. 29–35, Jan. 2018.
- [7] X. Shi, C. Yang, W. Xie, C. Liang, Z. Shi, and J. Chen, "Anti-drone system with multiple surveillance technologies: Architecture, implementation, and challenges," *IEEE Commun. Mag.*, vol. 56, no. 4, pp. 68–74, Apr. 2018.
- [8] F. Gökcge, G. Üçoluk, E. Şahin, and S. Kalkan, "Vision-based detection and distance estimation of micro unmanned aerial vehicles," *Sensors*, vol. 15, no. 9, pp. 23805–23846, Sep. 2015.
- [9] I. Bisio, C. Garibotto, F. Lavagetto, A. Sciarone, and S. Zappatore, "Unauthorized amateur UAV detection based on WiFi statistical fingerprint analysis," *IEEE Commun. Mag.*, vol. 56, no. 4, pp. 106–111, Apr. 2018.
- [10] Z. Shi, X. Chang, C. Yang, Z. Wu, and J. Wu, "An acoustic-based surveillance system for amateur drones detection and localization," *IEEE Trans. Veh. Technol.*, vol. 69, no. 3, pp. 2731–2739, Mar. 2020.
- [11] M. Z. Anwar, Z. Kaleem, and A. Jamalipour, "Machine learning inspired sound-based amateur drone detection for public safety applications," *IEEE Trans. Veh. Technol.*, vol. 68, no. 3, pp. 2526–2534, Mar. 2019.
- [12] L. Hauzenberger and E. H. Ohlsson, "Drone detection using audio analysis," M.S. thesis, Dept. Elect. Inf. Technol., Lund Univ., Lund, Sweden, 2015.
- [13] M. M. Azari, H. Sallouha, A. Chiumento, S. Rajendran, E. Vinogradov, and S. Pollin, "Key technologies and system trade-offs for detection and localization of amateur drones," *IEEE Commun. Mag.*, vol. 56, no. 1, pp. 51–57, Jan. 2018.
- [14] G. Fang, J. Yi, X. Wan, Y. Liu, and H. Ke, "Experimental research of multistatic passive radar with a single antenna for drone detection," *IEEE Access*, vol. 6, pp. 33542–33551, 2018.
- [15] J. Park, S. Park, D.-H. Kim, and S.-O. Park, "Leakage mitigation in heterodyne FMCW radar for small drone detection with stationary point concentration technique," *IEEE Trans. Microw. Theory Techn.*, vol. 67, no. 3, pp. 1221–1232, Mar. 2019.
- [16] L. S. C. D. Santos, L. A. D. Andrade, and A. M. Gama, "Analysis of radar cross section reduction of fighter aircraft by means of computer simulation," *J. Aerosp. Technol. Manage.*, vol. 6, no. 2, pp. 177–182, May 2014.
- [17] R. Nakamura and H. Hadama, "Characteristics of ultra-wideband radar echoes from a drone," *IEICE Commun. Exp.*, vol. 6, no. 9, pp. 530–534, 2017.
- [18] Á. D. de Quevedo, F. I. Urzaiz, J. G. Menoyo, and A. A. López, "Drone detection with X-band ubiquitous radar," in *Proc. 19th Int. Radar Symp. (IRS)*, Jun. 2018, pp. 1–10.

- [19] C. Zhao, C. Chen, Z. Cai, M. Shi, X. Du, and M. Guizani, "Classification of small UAVs based on auxiliary classifier Wasserstein GANs," in *Proc. IEEE Global Commun. Conf. (GLOBECOM)*, Dec. 2018, pp. 206–212.
- [20] I. Bisio, C. Garibotto, H. Haleem, F. Lavagetto, and A. Sciarrone, "On the localization of wireless targets: A drone surveillance perspective," *IEEE Netw.*, vol. 35, no. 5, pp. 249–255, Sep. 2021.
- [21] A. Bello, B. Biswal, S. Shetty, C. Kamhoua, and K. Gold, "Radio frequency classification toolbox for drone detection," in *Artificial Intelligence and Machine Learning for Multi-Domain Operations Applications*, vol. 11006. Bellingham, WA, USA: SPIE, 2019, pp. 689–704.
- [22] T. Boon-Poh, "RF techniques for detection, classification and location of commercial drone controllers," in *Proc. KeySight Technol., Aerosp. Defense Symp.*, 2017.
- [23] H. Lv, F. Liu, and N. Yuan, "Drone presence detection by the Drone's RF communication," *J. Phys., Conf.*, vol. 1738, no. 1, Jan. 2021, Art. no. 012044.
- [24] S. Yang, Y. Luo, W. Miao, C. Ge, W. Sun, and C. Luo, "RF signal-based UAV detection and mode classification: A joint feature engineering generator and multi-channel deep neural network approach," *Entropy*, vol. 23, no. 12, p. 1678, Dec. 2021.
- [25] F. Slimeni, T. Delleji, and Z. Chtourou, "RF-based mini-drone detection, identification and jamming in no fly zones using software defined radio," in *Proc. Int. Conf. Comput. Collective Intell.* Cham, Switzerland: Springer, Sep. 2022, pp. 791–798.
- [26] T. Huynh-The, Q.-V. Pham, T.-V. Nguyen, D. B. D. Costa, and D.-S. Kim, "RF-UAVNet: High-performance convolutional network for RF-based drone surveillance systems," *IEEE Access*, vol. 10, pp. 49696–49707, 2022.
- [27] E. Ozturk, F. Erden, and I. Guvenc, "RF-based low-SNR classification of UAVs using convolutional neural networks," 2020, *arXiv:2009.05519*.
- [28] O. O. Medaiyese, M. Ezuma, A. P. Lauf, and I. Guvenc, "Wavelet transform analytics for RF-based UAV detection and identification system using machine learning," *Pervas. Mobile Comput.*, vol. 82, Jun. 2022, Art. no. 101569.
- [29] B. Taha and A. Shoufan, "Machine learning-based drone detection and classification: State-of-the-art in research," *IEEE Access*, vol. 7, pp. 138669–138682, 2019.
- [30] M. Ezuma, F. Erden, C. K. Anjinappa, O. Ozdemir, and I. Guvenc, "Detection and classification of UAVs using RF fingerprints in the presence of Wi-Fi and Bluetooth interference," *IEEE Open J. Commun. Soc.*, vol. 1, pp. 60–76, 2020.
- [31] M. F. Al-Sa'd, A. Al-Ali, A. Mohamed, T. Khatat, and A. Erbad, "RF-based drone detection and identification using deep learning approaches: An initiative towards a large open source drone database," *Future Gener. Comput. Syst.*, vol. 100, pp. 86–97, Nov. 2019.
- [32] W. D. Scheller, "Detecting drones using machine learning," Ph.D. dissertation, Iowa State Univ., Ames, IA, USA, 2017.
- [33] P. Molchanov, R. I. A. Harmanny, J. J. M. de Wit, K. Egiazarian, and J. Astola, "Classification of small UAVs and birds by micro-Doppler signatures," *Int. J. Microw. Wireless Technol.*, vol. 6, nos. 3–4, pp. 435–444, Jun. 2014.
- [34] P. E. Pace, *Detecting and Classifying Low Probability of Intercept Radar*. Norwood, MA, USA: Artech House, 2009.
- [35] F. Hessar and S. Roy, "Spectrum sharing between a surveillance radar and secondary Wi-Fi networks," *IEEE Trans. Aerosp. Electron. Syst.*, vol. 52, no. 3, pp. 1434–1448, Jun. 2016.
- [36] Z. Weng, P. Orlik, and K. J. Kim, "Classification of wireless interference on 2.4 GHz spectrum," in *Proc. IEEE Wireless Commun. Netw. Conf. (WCNC)*, Apr. 2014, pp. 786–791.
- [37] T. Scholand and P. Jung, "Bluetooth receiver with zero-crossing zero-forcing demodulation," *Electron. Lett.*, vol. 39, no. 17, pp. 1275–1277, Aug. 2003.

- [38] J. Snoek, H. Larochelle, and R. P. Adams, "Practical Bayesian optimization of machine learning algorithms," in *Proc. Adv. Neural Inf. Process. Syst.*, vol. 25, 2012, pp. 3–7.
- [39] Y. V. Ahirrao, R. P. Yadav, and S. Kumar, "Design and development of RF-based unmanned aerial vehicle (UAV) detection system," in *Proc. IEEE Microw., Antennas, Propag. Conf. (MAPCON)*, Dec. 2023, pp. 1–4.



YASH VASANT AHIRRAO received the Bachelor of Engineering degree in electronics and telecommunication from North Maharashtra University, Jalgaon, India, in 2016.

He was a Junior Research Fellow with the Institute for Plasma Research, Gandhinagar, Gujarat, India, from May 2022 to May 2024, where he has been working, since June 2024, and is currently a Senior Research Fellow. During his tenure, he led the design and development of innovative RF-based UAV detection systems. His research interests include RF-based UAV detection systems, signal processing, and machine learning algorithms.



RANA PRATAP YADAV received the master's degree from the National Institute of Technology, Bhopal, India, in 2009, and the Ph.D. degree in high power RF engineering from the Homi Bhabha National Institute, Mumbai, India, in 2014.

During the Ph.D. degree, he was a Distinguished Fellow of the Department of Atomic Energy (DAE) and a Postdoctoral Fellow with the University of Oxford, U.K., from 2017 to 2018. He was an Assistant Professor with the Electronics and Communication Engineering Department, Thapar Institute of Engineering and Technology, from 2014 to 2021. He is currently an Assistant Professor with the Homi Bhabha National Institute and a Scientific Officer with the Institute for Plasma Research. With over nine years of experience, he has taught and supervised numerous students and received research grants from Indian agencies, such as BRNS-DAE, DST, and SERB. Specializing in RF/microwave systems design and fabrication, his research interests include high-power RF devices, antennas, RF plasma, RADAR, and navigation.



SUNIL KUMAR was born in Delhi, India, in March 1965. He received the bachelor's and master's degrees in physics from Delhi University, New Delhi, India, in 1985 and 1987, respectively, and the master's degree in microwave electronics from Delhi University (South Campus), New Delhi, in 1989. In 1990, he joined the Institute for Plasma Research, Gandhinagar, India, as a Radio Frequency Engineer, where he is currently the Head of the High Power ICRH Systems Division. His research interests include the development of high-power radio frequency amplifiers and oscillators and other equipment for plasma applications.

...